INSTITUTE OF PARASITOLOGY SAS KOŠICE

DOI 10.2478/helm-2025-0038

HELMINTHOLOGIA, 62, 4: 340 – 351, 2025

Immunomodulatory effects of *Terfezia claveryi* extract against experimental *Hysterothylacium thalassini* infection in mice

M. ALOTAIBI[1], R. ABDEL-GABER[1,*], S. AL QURAISHY[1], S. SANTOURLIDIS[2], H. M. ALHARBI[3], E. AL-SHAEBI[1]

[1]Department of Zoology, College of Science, King Saud University, P.O. 2455, Riyadh 11451, Saudi Arabia,
*E-mail: *rabdelgaber@ksu.edu.sa*; [2]Epigenetics Core Laboratory, Institute of Transplantation Diagnostics and Cell Therapeutics, Medical Faculty, Heinrich-Heine University Düsseldorf, Düsseldorf, Germany; [3]Department of Biology, College of Science, Princess Nourah bint Abdulrahman University, P.O. Box 84428, Riyadh 11671, Saudi Arabia

Article info

Received October 10, 2025
Accepted January 30, 2026

Summary

Fish are an essential source of high-quality protein and micronutrients. Yet parasitic infections often compromise safety. Anisakid nematodes, such as *Hysterothylacium thalassini*, are widely distributed in marine fish, including the greater lizardfish *Saurida tumbil*, and pose potential risks to human health. Infection with anisakid larvae is associated with oxidative stress, inflammatory responses, immune dysregulation, and apoptosis. Natural products rich in bioactive compounds may provide effective protection against these pathological effects. Desert truffles (*Terfezia claveryi*) possess well-documented antioxidant and immunomodulatory properties, but their activity against anisakid infections remains poorly characterized. This study investigated the protective effects of *Terfezia claveryi* extract (TCE) against experimental *H. thalassini* third-stage (L3) larval infection in a murine model, focusing on antioxidant activity, hematological changes, splenic immune responses, and Caspase-3-mediated apoptosis. TCE was prepared by methanol–water extraction, and its antioxidant potential was evaluated using the FRAP, DPPH, and ABTS assays. Forty male C57BL/6 mice were allocated into eight groups, including uninfected controls, TCE-treated mice, and mice infected with fresh, thermal, or frozen L3 larvae, with or without TCE treatment. After 14 days, hematological indices, spleen index, and Caspase-3 expression were assessed using immunohistochemistry, quantitative reverse transcription PCR, and ELISA. Larval infection induced significant anemia, leukocytosis, splenomegaly, and marked upregulation of Caspase-3, indicating enhanced oxidative stress and apoptotic activity. TCE administration significantly improved hemoglobin, red blood cell, hematocrit, platelet, and white blood cell values and reduced the spleen index. Caspase-3 expression was downregulated at both mRNA and protein levels, with ELISA-confirmed reductions in apoptotic markers (from 1178.37 ± 64.94 pg/mL in untreated infected mice to 744.79 ± 65.82 pg/mL following treatment). In conclusion, TCE exhibits potent antioxidant, anti-apoptotic, and immunomodulatory effects that alleviate *H. thalassini*-induced hematological and splenic alterations, supporting its potential as a natural therapeutic candidate against fishborne parasitic infections globally.

Keywords: Fishborne zoonoses; Anisakids; natural products; truffles; immunomodulation; apoptosis

Introduction

Fish are widely considered an important part of a healthy diet because they provide high-quality protein, essential amino acids, polyunsaturated fatty acids—particularly omega-3s—and a variety of micronutrients, including vitamins A, D, B12, selenium, and iodine.

* – corresponding author

These nutrients are essential for supporting human growth, neurological development, cardiovascular health, and proper immune function. However, despite these nutritional benefits, fish are frequently susceptible to a variety of parasitic infections, which pose serious challenges to food safety, public health, and the economic viability of fisheries (Dela Cruz *et al*., 2022).

Anisakid nematodes, including *Anisakis*, *Pseudoterranova*, *Contracaecum*, and *Hysterothylacium*, are a major group of parasites of concern in fish. These nematodes are common in marine ecosystems and follow complex life cycles involving multiple hosts, such as fish and marine mammals. Accidental human infection can occur after ingesting raw or undercooked fish containing third-stage larvae (L3). Anisakiasis in humans represents an increasingly important zoonotic condition, manifesting as gastrointestinal disturbances (nausea, vomiting, abdominal pain, and diarrhea) together with allergic reactions that range from urticaria to anaphylaxis. In addition, dysregulated immune responses, including eosinophilia and Th2-mediated inflammation, can aggravate tissue injury and prolong disease recovery (Audicana *et al*., 2022; Chai *et al*., 2024).

The greater lizardfish (*Saurida tumbil*), a commercially valuable species in the Red Sea and Arabian Gulf, is commonly infected with the anisakid nematode parasite of *Hysterothylacium thalassini* larvae (Li *et al*., 2007). Infection in these fish not only diminishes food quality and marketability but also triggers oxidative stress and immune perturbations in the host. Specifically, immune cells such as eosinophils, macrophages, and T helper 2 (Th2) lymphocytes are activated, producing reactive oxygen species (ROS), proinflammatory cytokines, and additional inflammatory mediators. This process can intensify tissue injury and cellular damage, ultimately contributing to organ dysfunction and systemic stress (Menshawy *et al*., 2024).

With growing concern about drug resistance and the scarcity of pharmacological options for managing parasitic infections, natural bioactive compounds with antioxidant and immunoprotective properties have attracted increasing attention. Desert truffles, especially *Terfezia claveryi*, have gained attention as a promising natural candidate. They are abundant in phenolic acids, flavonoids, polysaccharides, and other secondary metabolites that confer various bioactivities, including antioxidant, anti-inflammatory, antimicrobial, and immunomodulatory effects (Janakat & Nassar, 2010; İşlek *et al*., 2021). In regions such as Saudi Arabia, *T. claveryi*—locally referred to as "kamma"—is traditionally consumed not only as a culinary specialty but also for its medicinal properties against infections and inflammation, reflecting its combined nutritional and therapeutic significance (Veeraraghavan *et al*., 2021). Leveraging natural bioactive agents in strategies to prevent or treat fishborne parasitic infections may offer a safer, more sustainable option than standard chemical interventions.

Given the limited pharmacological options for controlling anisakid infections and the immunotoxic effects of parasite-induced oxidative stress, this study investigates the protective effects of *T. claveryi* extract (TCE) against experimental *H. thalassini* L3 infection in a mouse model. The study focuses on hematological and splenic immune parameters—including leukocyte profiles, cytokine regulation, and Caspase-3 expression—to assess TCE's potential as a natural antioxidant and immunomodulatory agent.

Materials and Methods

Collection of Terfezia claveryi

Fresh brown desert truffles (*Terfezia claveryi*, locally termed as *kamma*) were harvested from the Al-Mashaliyah Reserve in Tulayhah, Saudi Arabia (27°41'78" N, 43°17'36" E). The specimens were taxonomically verified by experts at the Herbarium of the Botany Department, King Saud University (Riyadh, Saudi Arabia), where voucher specimens were deposited for future reference.

Preparation of T. claveryi extract (TCE)

The fruiting bodies of *T. claveryi* were washed with distilled water, cut into small pieces, and then air-dried in the shade at room temperature. The dried material was ground into a fine powder using a Hummer grinder (ED-CG1400). Following Souna *et al*. (2023), 100 g of the powder was macerated in a 70:30 (v/v) methanol–water mixture for 2 hr with continuous shaking at room temperature, then stored at 4°C for 48 hr to optimize extraction. The mixture was filtered through Whatman paper, and the filtrate was concentrated under reduced pressure at 40°C using a rotary evaporator (Buchi, Switzerland). The concentrated extract was freeze-dried to yield a dry powder, which was stored at −20°C until reconstitution in distilled water for subsequent analyses. No targeted phytochemical profiling or compound-specific identification (e.g., HPLC or LC–MS analysis) was performed in the present study, and the extract was evaluated as a whole for its biological activity.

Ferric reducing antioxidant power (FRAP) assay

The total antioxidant capacity of the samples was assessed using the FRAP assay, following Benzie & Strain (1996) with minor modifications. The method relies on the reduction of the ferric (Fe^{3+})–TPTZ complex to its ferrous (Fe^{2+}) form by antioxidants under acidic conditions, producing a blue-colored complex that is measured spectrophotometrically at 593 nm. The FRAP reagent was freshly prepared by mixing 300 mM acetate buffer (pH 3.6), 10 mM TPTZ solution in 40 mM HCl, and 20 mM $FeCl_3 \cdot 6H_2O$ solution in a 10:1:1 (v/v/v) ratio. A calibration curve was constructed using $FeSO_4 \cdot 7H_2O$ standard solutions (100 – 1000 µM). For the assay, 100 µL of the extract (1 mg/mL) was mixed with 3 mL of the FRAP reagent and incubated at 37°C in the dark for 30 min. The absorbance of the resulting ferrous–TPTZ complex was recorded at 593 nm using a UV–visible spectrophotometer against a reagent blank. The antioxidant capacity was calculated from the standard curve and expressed as micromoles of Fe^{2+} equivalents per gram of sample (µmol Fe^{2+}/g).

Free radical scavenging activity (DPPH assay)

The 2,2-diphenyl-1-picrylhydrazyl (DPPH) assay was conducted to evaluate the extract's free radical scavenging activity, following Baliyan *et al*. (2022) with minor modifications. In brief, 200 µL of the extract was combined with 1.8 mL of 0.2 mM methanolic DPPH solution and thoroughly mixed. The mixture was then incubated in the dark at room temperature for 30 min to allow complete interaction between antioxidants and DPPH radicals. The absorbance was then measured at 517 nm using a UV–visible spectrophotometer against a methanol blank. DPPH free radical scavenging activity was calculated according to the following equation: % DPPH radical scavenging activity = $(Abs_{control}–Abs_{sample}) / (Abs_{control}) \times 100$. Where $Abs_{control}$ is the absorbance of DPPH radical + methanol; Abs_{sample} is the absorbance of DPPH radical + sample extract. The IC_{50} value, defined as the concentration of the extract required to scavenge 50 % of DPPH radicals, was obtained from the linear regression of the inhibition percentage plotted against extract concentration.

ABTS radical scavenging assay

The antioxidant capacity of the samples was assessed using the ABTS [2,2'-azinobis-(3-ethylbenzothiazoline-6-sulfonic acid)] radical cation scavenging assay, following Re *et al*. (1999) with minor modifications. This method is based on antioxidants' ability to neutralize the blue-green $ABTS^{+}$• radical cation, resulting in a decrease in absorbance at 734 nm. The $ABTS^{+}$• working solution was prepared by reacting 7 mM ABTS with 2.45 mM potassium persulfate ($K_2S_2O_8$) and incubating in the dark at room temperature for 12 – 16 hr. The solution was then diluted with ethanol or phosphate-buffered saline (PBS) to an absorbance of 0.70 ± 0.02 at 734 nm. For the assay, 100 µL of the extract was added to 3 mL of the $ABTS^{+}$• solution and incubated in the dark at room temperature for 6 min. The reduction in absorbance was measured at 734 nm, and radical-scavenging activity was calculated relative to the control. Trolox served as the reference standard, and the results were expressed as Trolox equivalent antioxidant capacity (TEAC, µmol Trolox equivalents per gram of sample).

Fish and parasite collection

Thirty specimens of the greater lizardfish, *Saurida tumbil* (family: Synodontidae), were obtained from fish markets in Jeddah, Saudi Arabia (Red Sea), and transported to the Laboratory of Parasitology for further analysis. During dissection, the visceral cavity and digestive tract of each fish were examined macroscopically for third-stage larvae (L3), as shown in Figure 1, following Abdel-Gaber *et al*. (2024). Recovered larvae were carefully collected and repeatedly washed with phosphate-buffered saline (PBS) to remove any debris. The larvae were then divided into three treatment

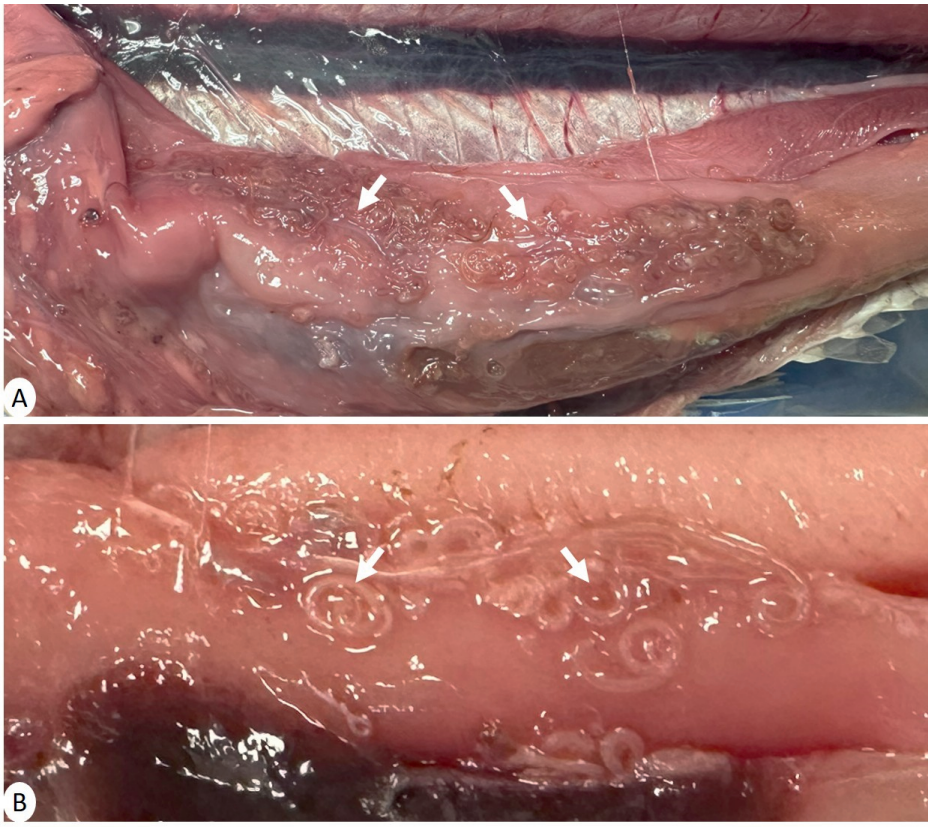

Fig. 1. (A and B) Third-stage larvae (white arrow) for the nematode parasite, *H. thalassini*, in the peritoneal cavity of *S. tumbil*.

groups: (i) **Fresh L3**, maintained at room temperature (~23°C) for 60 min; (ii) **Thermal L3**, exposed to a water bath at 100°C for 60 min; and (iii) **Frozen L3**, stored at −20°C for 24 hr. Crude larval extracts were prepared before inoculation by homogenizing twenty portions (approximately 10 larvae per mouse) of each treatment group. Larvae of similar size were disrupted using microtube pestles and subjected to ultrasonic homogenization on ice at 100 W for five cycles of 30 sec each (Iglesias *et al*., 1996). The homogenate was centrifuged at 3000 rpm for 15 min at 4°C, and the supernatant was collected for subsequent experimental procedures.

Experimental animals

Male C57BL/6 mice (n = 40), aged 9 – 12 weeks and weighing 20 – 25 g, were used in this study. The animals were obtained from the College of Pharmacy's animal facility at King Saud University. Mice were housed in polypropylene cages, with five animals per cage, under controlled environmental conditions (23 ± 2°C) and a 12-hr light/12-hr dark cycle. Before the experiments began, the mice were acclimated for one week. Standard laboratory chow and water were provided *ad libitum* throughout the study.

Experimental design

Forty male C57BL/6 mice were randomly assigned into eight groups (n = 5 per group) as follows: **Group I (Control):** received saline orally for 14 days. **Group II (TCE):** received TCE alone at 250 mg/kg orally for 14 days (Abbas, 2019). **Group III (Fresh L3):** inoculated with crude extract of fresh third-stage larvae (L3) on days 0 and 7. **Group IV (Thermal L3):** inoculated with crude extract of thermally treated L3 on days 0 and 7. **Group V (Frozen L3):** inoculated with crude extract of frozen L3 on days 0 and 7. **Group VI (Fresh L3 + TCE):** received TCE (250 mg/kg) for 14 days and inoculated with fresh L3 crude extract on days 0 and 7. **Group VII (Thermal L3 + TCE):** received TCE for 14 days and inoculated with thermally treated L3 crude extract on days 0 and 7. **Group VIII (Frozen L3 + TCE):** received TCE for 14 days and inoculated with frozen L3 crude extract on days 0 and 7. This experimental setup enabled the evaluation of the protective and therapeutic effects of TCE under different L3 treatment conditions.

Sample collection

On day 14, mice were humanely euthanized, and dissections were performed to obtain the necessary samples. Blood was collected via cardiac puncture into heparinized tubes for subsequent analyses. The spleen was carefully removed, cut into small sections, and preserved for different purposes: (i) fixation in neutral buffered formalin (NBF) for immunohistochemical studies, and (ii) immersion in RNAlater for gene and protein expression studies, followed by storage at −80°C until use.

Immuno-hematological parameters

Key blood parameters—including red blood cells (RBCs), hemoglobin (Hb), hematocrit (HCT), platelets, and white blood cells (WBCs)—were measured in each mouse. Analyses were conducted using a veterinary hematology analyzer (VET-530, CA Medonic; Medonic, Stockholm, Sweden) according to Dkhil *et al*. (2023). This method enabled precise quantification of blood cell components and assessment of hematological responses to the experimental treatments.

Spleen index

Each mouse's spleen was removed and weighed, and the body weight of the corresponding animal was recorded. The spleen index, representing the spleen's size relative to body weight, was calculated using the formula from Bauomy *et al*. (2014): Spleen index = (spleen weight in milligrams) / (mouse body weight in grams). This index indicates splenic enlargement or atrophy and reflects the physiological and immune status of the mice in each experimental group.

Immunohistochemical examination

Spleen samples were fixed in 10 % neutral buffered formalin (NBF) for 24 hr. The tissues were dehydrated through a graded ethanol series, cleared in xylene, embedded in paraffin, and sectioned at 5 µm using a microtome. Sections were deparaffinized in xylene, rehydrated through descending ethanol concentrations (100 %, 96 %, 70 % v/v), and then rinsed in distilled water. Antigen retrieval was conducted in 0.01 M citrate buffer, with incubation conditions optimized for the specific antibody. Sections were then washed with phosphate-buffered saline (PBS, pH 7.4), treated with 3 % H2O2 for 5 min to quench endogenous peroxidase activity, and then washed again with PBS. Prepared sections were incubated overnight at 4°C with primary antibodies, including cysteine-aspartic acid protease-3 (Caspase-3; R&D Systems, Minneapolis, USA), while control sections were treated with 2 % bovine serum albumin (BSA). Following PBS washes, immunohistochemical detection was carried out using the streptavidin-biotin complex (Strept-ABC) method. All sections were counterstained with hematoxylin-eosin (H&E), rinsed under running tap water, dehydrat-

Table 1. Oligonucleotide primer sequences for reverse transcription PCR amplification in the experiment.

RNA target	Direction	Oligonucleotide sequence (5'-3')	NCBI reference
Caspase-3	Forward	CTAGCAGGATCCAGCAGTCC	NM_009810
	Reverse	CCCCTATTCCACCCAACTTT	
β-actin	Forward	GCTACAGCTTCACCACCACA	NM_007393
	Reverse	AAGGAAGGCTGGAAAAGAGC	

ed in ascending ethanol series (70 %, 96 %, 100 % v/v), cleared in xylene, and mounted using Canada balsam. Stained sections were examined and photographed using a Leica DM2500 microscope with NIS-Elements software (version 3.8), allowing detailed observation of tissue morphology and antigen expression.

Gene expression analysis

Spleen tissues were processed for total RNA extraction using TRIzol reagent (Invitrogen) according to the manufacturer's instructions. The isolated RNA was treated with DNase I (Applied Biosystems, Darmstadt, Germany) for at least 1 hr to remove contaminating genomic DNA and subsequently reverse-transcribed into cDNA using a reverse transcription kit (Qiagen, Hilden, Germany). Quantitative real-time PCR (qRT-PCR) was performed on an ABI Prism 7500HT sequence detection system (Applied Biosystems, Darmstadt, Germany) using SYBR Green PCR Master Mix (Qiagen, Hilden, Germany). Caspase-3 was selected as the target gene, and primers were obtained from Qiagen (Table 1). Beta-actin (β-actin) was used as the endogenous reference gene. Amplification and data analysis were carried out using the Applied Biosystems StepOne™ software (version 3.1, USA). Relative gene expression levels were calculated using the comparative Ct ($2^{-\Delta\Delta Ct}$) method as described by Livak & Schmittgen (2001).

Sandwich enzyme-linked immunosorbent assay (ELISA)

Caspase-3 concentrations in spleen tissue were quantified using a mouse-specific ELISA kit according to the manufacturer's protocol to ensure reliable, reproducible results. Briefly, tissue homogenates were prepared, and the assay was performed according to the recommended incubation and washing procedures. Optical densities (OD) were recorded using a Bio-Rad iMark Microplate Reader (software version 1.04.02.E), as outlined by Al-Quraishy *et al*. (2024). Caspase-3 concentrations were quantified by relating sample OD values to a standard calibration curve and expressed in picograms per milliliter (pg/mL), allowing precise measurement of protein concentrations.

Statistical analysis

Data are expressed as mean ± standard deviation (SD) to indicate variability within each group. Differences among groups were evaluated using one-way analysis of variance (ANOVA) performed with SPSS software (version 18; SPSS Inc., Chicago, IL, USA). Following ANOVA, Tukey's honestly significant difference (HSD) post-hoc test was applied for pairwise group comparisons. A p-value of ≤0.05 was considered statistically significant for all comparisons.

Ethical Approval and/or Informed Consent

This study was reviewed and approved by the Research Ethics Committee (REC) of King Saud University, Riyadh, Saudi Arabia (approval number KSU-SE-25-28). The approval ensures that all animal experiments were conducted in compliance with institutional guidelines for laboratory animal care and in accordance with international ethical standards.

Results

The antioxidant activity of TCE was further validated using multiple *in vitro* assays (Table 2). The extract demonstrated a ferric reducing antioxidant power (FRAP) of 87.15 ± 2.34 µmol/g, reflecting strong electron-donating and reducing capabilities. Its free radical scavenging activity, assessed by the DPPH assay, reached 76.21 ± 1.37 %, indicating effective neutralization of stable free radicals. The ABTS assay showed even higher activity, at 97.20 ± 0.27 µmol/g, confirming that TCE exhibits potent radical-scavenging activity across different oxidative systems. The antioxidant capacity observed reflects the cumulative redox activity of the crude extract and does not allow attribution to individual phytochemical constituents.

Anemia in mice was evaluated using key hematological parameters, including hemoglobin concentration, red blood cell count, and hematocrit (Table 3). Uninfected control mice exhibited an average hemoglobin level of 13.24 ± 0.61 g/dL. In contrast, infected groups showed significant reductions: 8.86 ± 0.35 g/dL for mice exposed to fresh L_3 larvae, 9.76 ± 0.35 g/dL for those infected with thermally processed L_3, and 9.42 ± 0.28 g/dL for mice infected with frozen L_3 (Table 3). These significant differences indicate a considerable degree of anemia among the infected cohorts. Similarly, the erythrocyte counts further underscore the severity of anemia caused by the L_3 infection (Table 3). The control group's erythrocyte count was 10.34 ± 0.86 million red blood cells (RBCs) per mm³. However, this count was significantly lower in the infected groups, with only 7.79 ± 0.27 million RBCs per mm³ recorded in mice exposed to fresh L3 and counts of 8.78 ± 0.34 million RBCs per mm³ and 8.35 ± 0.12 million RBCs per mm³ in those infected with thermally processed and frozen L_3, respectively. In an effort to ameliorate the anemia, mice infected with L_3 larvae were treated with TCE.

Table 2. Phytochemical composition and antioxidant activity of *Terfezia claveryi* extract (TCE), including FRAP, DPPH, and ABTS assays.

Phytochemical	FRAP (µmol/g)	DPPH (%)	ABTS (µmol/g)
Qualitative	+++	+++	+++
Quantitative	87.15 ± 2.34	76.21 ± 1.37	97.20 ± 0.27

-: absent; +: low; ++: moderate; +++: high

Table 3. TCE caused changes in hematological parameters of mice's blood after L_3 infection.

Experimental mouse groups		Red blood cells ($\times 10^6$/l)	Hemoglobin (g/dl)	Hematocrit (%)	Platelets ($\times 10^3$/L)	White blood cells ($\times 10^3$/L)
Control		10.34 ± 0.86	13.24 ± 0.61	47.06 ± 5.32	328.67 ± 24.68	5.56 ± 0.64
TCE		10.49 ± 0.90	13.22 ± 0.51	46.57 ± 4.37	345.67 ± 11.67	5.35 ± 0.72
Infected	Fresh L_3	7.79 ± 0.27*	8.86 ± 0.35*	31.10 ± 1.15*	858.33 ± 31.13*	19.63 ± 1.01*
	Thermal L_3	8.78 ± 0.34*	9.76 ± 0.35*	36.90 ± 1.80*	613.33 ± 46.32*	10.43 ± 0.75*
	Frozen L_3	8.35 ± 0.12*	9.42 ± 0.28*	35.36 ± 2.28*	649.67 ± 18.61*	10.96 ± 0.31*
Infected-TCE	Fresh L_3	8.67 ± 0.52*#	9.90 ± 0.26*#	38.47 ± 2.05*#	558.67 ± 35.85*#	9.03 ± 0.60*#
	Thermal L_3	9.80 ± 0.47*#	11.90 ± 0.36*#	42.46 ± 0.93*#	453.67 ± 14.18*#	7.83 ± 0.15*#
	Frozen L_3	9.48 ± 0.32*#	10.90 ± 0.30*#	40.70 ± 1.41*#	487.00 ± 18.52*#	8.07 ± 0.25*#

* denotes a statistically significant difference relative to the control group; # denotes a statistically significant difference relative to the infected group.

The results indicated a positive hematological response following TCE treatment, as reflected by increased hemoglobin levels (Table 3). In mice infected with fresh L_3, hemoglobin rose to 9.90 ± 0.26 g/dL. Those treated with thermally processed L_3 exhibited a greater improvement, reaching 11.90 ± 0.36 g/dL, while frozen L_3-infected mice showed an increase to 10.90 ± 0.30 g/dL. Similarly, erythrocyte counts increased after treatment: 8.67 ± 0.52 million RBCs per mm³ for fresh L_3, 9.80 ± 0.47 million RBCs per mm³ for thermally processed L_3, and 9.48 ± 0.32 million RBCs per mm³ for frozen L_3. Hematocrit values, another key indicator of anemia, remained lower in the infected groups than in controls, averaging 47.06 ± 5.32 (Table 3). The infected groups showed compromised values of 31.10 ± 1.15 % for those exposed to fresh L_3, 36.90 ± 1.80 % for those exposed to thermally processed L3, and 35.36 ± 2.28 % for those exposed to frozen L_3. In contrast, post-TCE treatment, hematocrit percentages improved to 38.47 ± 2.05 % for fresh L_3, 42.46 ± 0.93 % for thermally processed L_3, and 40.70 ± 1.41 % for frozen L_3, highlighting TCE's potential to mitigate anemia.

Additionally, significant changes were noted in platelet counts across the infected groups (Table 3). The average platelet count reached 858.33 ± 31.13 million platelets per mm³ in the group infected with fresh L_3. This was further observed as 613.33 ± 46.32 million platelets per mm³ in the thermally processed L3 group and 649.67 ± 18.61 million platelets per mm³ in the frozen L_3 group. For comparison, the control group exhibited a baseline platelet count of

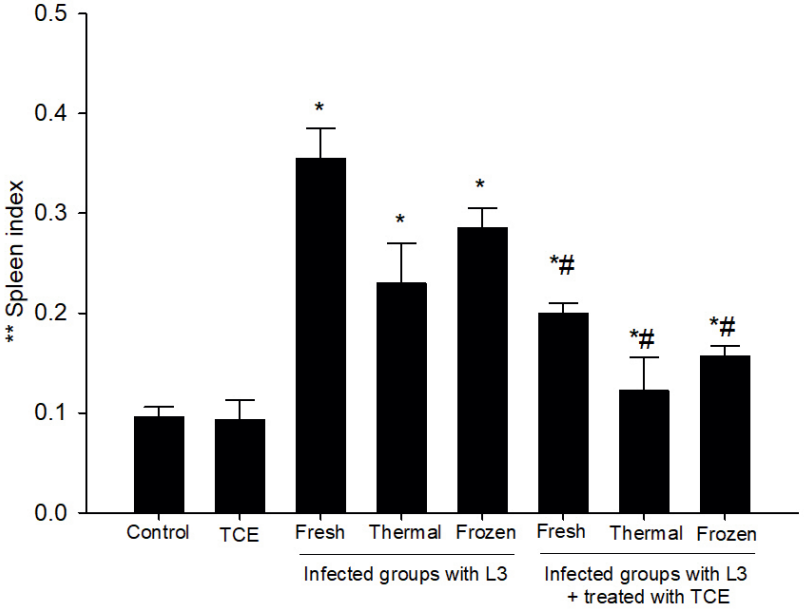

Fig. 2. Changes in the spleen index of the spleen of uninfected, infected with fresh, thermally, and frozen L_3 larvae, as well as in infected groups administered TCE (250 mg/kg).
* denotes a statistically significant difference relative to the control group; # denotes a statistically significant difference relative to the infected group.
** Ratio of spleen weight in mg/mouse to body weight in g/mouse.

only 328.67 ± 24.68 million platelets per mm³. However, following TCE treatment, platelet counts significantly declined, with values dropping to 558.67 ± 35.85 million platelets per mm³ for fresh L_3, 453.67 ± 14.18 million platelets per mm³ for thermally processed L_3, and 487.00 ± 18.52 million platelets per mm³ for frozen L_3. Conversely, the infected groups exhibited a pronounced increase in white blood cell (WBC) counts, averaging 19.63 ± 1.01 million WBCs per mm³ in mice exposed to fresh L_3 (Table 3). In the thermally processed L_3 and frozen L_3 groups, the WBC counts were 10.43 ± 0.75 million per mm³ and 10.96 ± 0.31 million per mm³, respectively, compared to the control group's count of 5.56 ± 0.64 million WBCs per mm³. Notably, TCE treatment resulted in a significant decrease in WBC counts, which were measured at 9.03 ± 0.60 million WBCs per mm³ for fresh L_3, 7.83 ± 0.15 million WBCs per mm³ for thermally processed L_3, and 8.07 ± 0.25 million WBCs per mm³ for frozen L_3, indicating the treatment's efficacy in modulating the immune response following infection.

The spleen index, expressed as the ratio of spleen weight to body weight, was used as an indicator of splenic enlargement and pathological changes among the different experimental groups. A statistically significant elevation in spleen index values was observed in all infected groups when compared with the uninfected control group (Fig. 2). Mice infected with fresh L_3 larvae showed the most severe splenomegaly, with a spleen index of 0.35 ± 0.03. Infections with thermally processed and frozen L_3 larvae also increased spleen indices to 0.23 ± 0.04 and 0.26 ± 0.02, respectively, though slightly lower than in the fresh L_3 group. Notably, TCE treatment significantly reduced infection-induced splenic enlargement in all groups. The spleen index decreased to 0.20 ± 0.01 in fresh L_3-infected mice, and to 0.12 ± 0.03 and 0.16 ± 0.01 in the thermally processed and frozen L_3 groups, respectively. These results underscore the protective effect of TCE in alleviating parasite-induced splenic hypertrophy and its potential to counteract infection-related pathological changes.

Spleen sections from different experimental mouse groups were processed and stained to evaluate caspase-3 expression, a key regulator of apoptosis (Fig. 3). Results showed that L_3 infection significantly increased caspase-3 levels, indicating enhanced activation of apoptotic pathways. Mice infected with fresh L_3 exhibited extensive immunostaining, with numerous cells positive for caspase-3, followed by those infected with frozen and thermally treated L_3. In contrast, control mice displayed baseline staining levels (Fig. 3). These findings reveal a marked pathological effect of L_3 infection, as the accumulation of caspase-3-positive cells deviated substantially from normal, suggesting that L_3 induces apoptosis, likely via activation of intrinsic apoptotic signaling. Additionally,

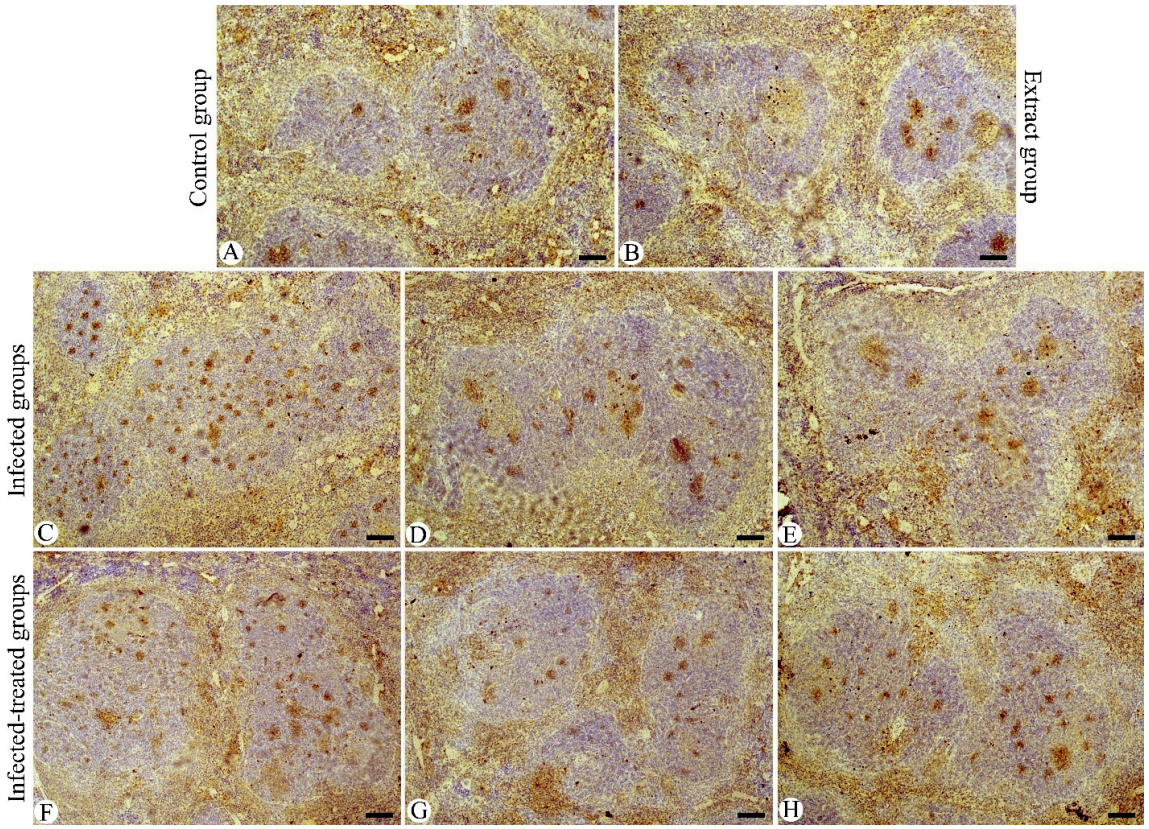

Fig. 3. Immunohistochemical detection of caspase-3 in the spleen of mice. (A) control group. (B) *Terfezia claveryi* extract (TCE)-treated group. (C–E) infected groups with fresh, thermally, and frozen L_3, respectively. (F–H) infected-treated groups with TCE (250 mg/kg) after inoculation with fresh, thermally, and frozen L_3, respectively. Scale bar = 50 µm.

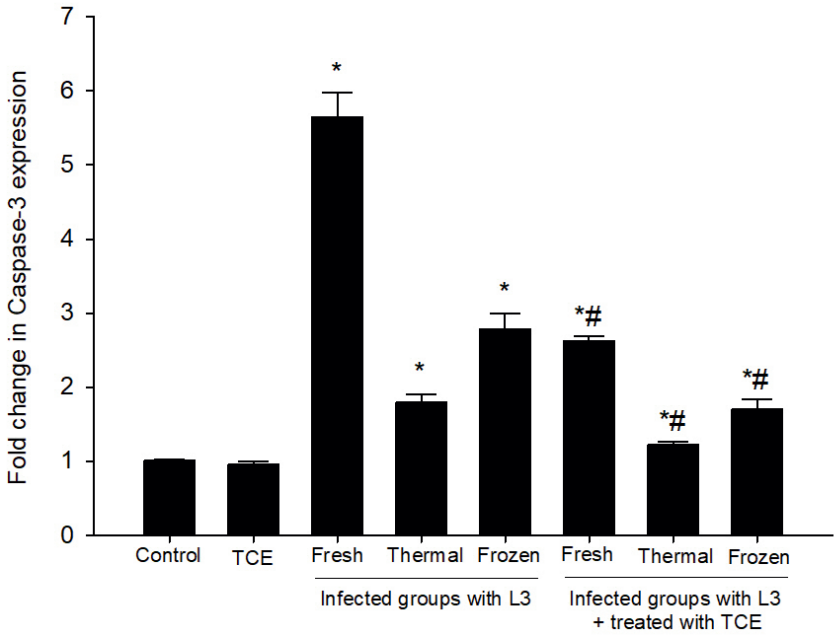

Fig. 4. Effect of TCE on the mRNA expression of Caspase-3 in the spleen samples from L_3-infected mice. The RT-PCR expression values were normalized to the reference gene β-actin and expressed as fold induction (log2 scale) relative to the control.
* denotes a statistically significant difference relative to the control group; # denotes a statistically significant difference relative to the infected group.

after treatment, a significant change in caspase-3 expression levels was noted. The infected and treated groups that received TCE showed only mild caspase-3 immunostaining, particularly in those infected with thermally treated L3, compared with the higher levels observed in the untreated infected groups. The marked reduction in caspase-3 expression highlights the potential of therapeutic interventions to modulate and suppress apoptosis induced by L_3 infection, indicating promising directions for future research on strategies to mitigate infection-related effects.

Infection with the L_3 larvae resulted in a significant upregulation of Caspase-3 mRNA expression. Specifically, expression levels increased by approximately 5.65-fold when mice were exposed to fresh L_3 larvae. In contrast, the increase was somewhat reduced to 1.79-fold for those infected with thermally processed L_3 larvae, while a 2.78-fold increase was observed in mice infected with frozen L_3 larvae. These findings were compared with a control group set at a baseline expression level of 1.00-fold, serving as a reference (Fig. 4). Following TCE treatment, a notable decrease in Caspase-3 mRNA expression was observed across all treatment groups. After TCE intervention, expression levels dropped to approximately 2.62-fold for the group infected with fresh L3, 1.21-fold for those with thermally processed L3, and 1.69-fold for mice infected with frozen L_3 larvae. This marked reduction indicates that TCE played a significant role in modulating the inflammatory response initiated by the infection, leading to reduced Caspase-3 gene expression. These findings highlight the potential of TCE as a therapeutic agent for controlling inflammation linked to L_3 larval infections (Fig. 4).

This study investigated the effects of TCE on apoptosis during infection and its potential role in modulating inflammatory responses. Caspase-3, a key executor of apoptosis, was measured by Enzyme-Linked Immunosorbent Assay (ELISA), with results shown in Figure 5. L_3 infection led to a significant increase in caspase-3 levels, reaching 1178.37 ± 64.94 pg/ml in mice infected with fresh L_3 larvae. In contrast, infection with thermally processed L_3 elicited a lower caspase-3 level of 495.35 ± 25.42 pg/ml, while those infected with frozen L_3 demonstrated intermediate levels of 652.97 ± 124.71 pg/ml. These results were statistically significant compared with baseline control levels, demonstrating that L_3 infection markedly elevates the apoptotic response. Intriguingly, when the mice were treated with TCE, a pronounced reduction in the L_3-induced elevations of caspase-3 levels was observed. Specifically, caspase-3 levels were reduced to 744.79 ± 65.82 pg/ml in those subjected to fresh L3 after TCE treatment, whereas thermally processed L_3 infections resulted in even lower levels of 375.06 ± 10.38 pg/ml. Additionally, mice infected with frozen L_3 exhibited decreased caspase-3 levels, measured at 490.75 ± 33.54 pg/ml following TCE treatment. These results strongly indicate that TCE effectively mitigates L_3-induced apoptosis, highlighting its potential as a therapeutic agent managing infections and related inflammatory responses.

Discussion

Parasitic infections are known to induce complex physiological disturbances, including oxidative stress, hematological imbalances,

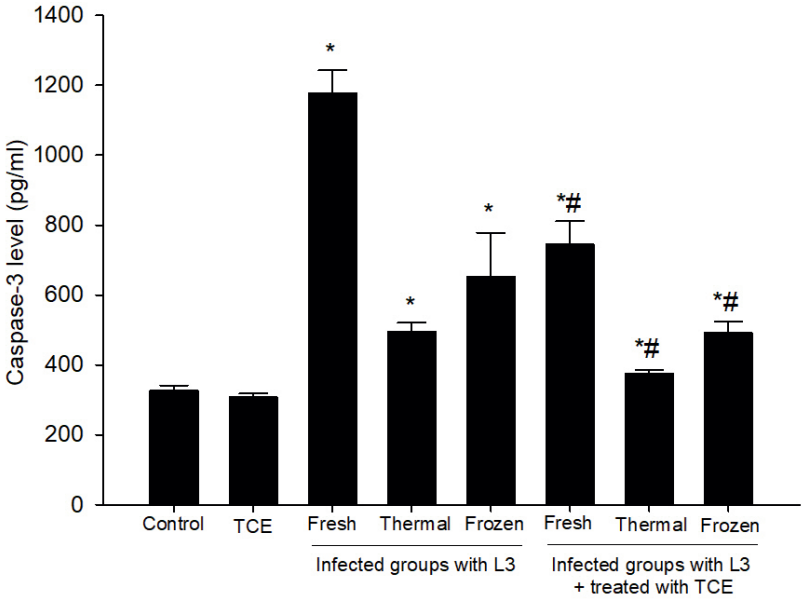

Fig. 5. Caspase-3 level in the spleen samples from the different experimental mouse groups.
* denotes a statistically significant difference relative to the control group; # denotes a statistically significant difference relative to the infected group.

and immune dysregulation, emphasizing the need for natural therapeutic agents with broad protective effects (Elsayed *et al*., 2019; Pawłowska *et al*., 2023). This study provides strong experimental evidence that TCE possesses significant antioxidant, hematoprotective, immunomodulatory, and anti-apoptotic activities against *H. thalassini* L3–induced oxidative and pathological changes. Biochemical, hematological, histological, and molecular analyses demonstrated that TCE effectively alleviates infection-induced oxidative stress, ameliorates anemia, restores immune cell balance, and inhibits apoptosis-related signaling pathways in mice. Collectively, these results highlight TCE's potential as a natural bioactive agent that can counteract the multifaceted pathophysiological effects of parasitic infections.

In vitro antioxidant assays, including FRAP, DPPH, and ABTS, clearly demonstrated TCE's remarkable redox activity. The extract showed strong electron-donating and hydrogen atom transfer (HAT) capacities, reflecting its effectiveness in neutralizing various reactive oxygen species (ROS) and maintaining cellular redox balance. These results suggest that TCE is rich in bioactive phytochemicals, particularly polyphenols and flavonoids, which stabilize free radicals via resonance delocalization and redox cycling (Al-Laith, 2010; Tejedor-Calvo *et al*., 2021). Such compounds scavenge hydroxyl, superoxide, and peroxyl radicals and chelate transition metals like Fe^{2+} and Cu^{2+}, thereby preventing Fenton-type reactions. Additionally, TCE enhances the activity and expression of endogenous antioxidant enzymes, including superoxide dismutase (SOD), catalase (CAT), and glutathione peroxidase (GPx), strengthening the cellular defense system and reducing lipid peroxidation. The potent *in vitro* antioxidant activity of TCE provides a mechanistic basis for its *in vivo* efficacy, suggesting that its phenolic constituents synergistically counteract infection-induced oxidative stress, suppress inflammatory pathways, and protect cellular integrity during *H. thalassini* L3 infection. Although previous studies of Kivrak *et al.* (2019), Souna *et al.* (2023), and Guenane *et al.* (2024) have identified phenolic acids and flavonoids as major contributors to the antioxidant activity of *T. claveryi*, the present study did not directly characterize these compounds, and thus their involvement should be interpreted as presumptive rather than definitive.

In the present study, the immunomodulatory effects of *T. claveryi* extract were evaluated through indirect but biologically relevant indicators of immune function, including hematological leukocyte profiles, spleen index alterations, and regulation of apoptosis-related signaling in splenic tissue. These parameters reflect modulation of immune-associated physiological responses, particularly immune cell activation, proliferation, and survival, rather than comprehensive immune pathway analysis. Accordingly, the term 'immunomodulatory' is used in this study to describe the extract's capacity to attenuate infection-induced immune dysregulation and tissue-level immune stress, rather than to denote direct effects on specific cytokines, immune receptors, or signaling cascades.

Hematological evaluation of mice infected with *H. thalassini* L3 revealed significant impairments in red blood cell parameters, including reduced hemoglobin concentration, erythrocyte count, and hematocrit, consistent with normocytic, normochromic anemia. These changes reflect parasite-induced hematotoxicity arising from multiple mechanisms, such as direct mechanical damage to erythrocytes, ROS-mediated oxidative hemolysis, and suppression of bone marrow erythropoiesis via inflammatory cytokines and oxidative stress (Bernal-Valle *et al*., 2022; Al Quraishy *et al*., 2024).

Additional contributors include splenic sequestration of damaged RBCs and disruption of iron metabolism during systemic infection. Treatment with TCE markedly alleviated these hematological disturbances, restoring hemoglobin, RBC counts, and hematocrit toward normal levels. This protective effect is likely attributed to TCE's rich polyphenolic and flavonoid content, which exerts strong antioxidant activity, stabilizes erythrocyte membranes, prevents lipid peroxidation, and may support erythropoiesis by modulating oxidative stress and cytokine-mediated regulation of erythroid progenitor proliferation, ultimately leading to hematological recovery in infected mice.

Beyond red blood cell alterations, *H. thalassini* L3 infection led to marked leukocytosis and thrombocytosis in mice, evidenced by elevated WBC and platelet counts, which reflect systemic inflammatory activation and immune mobilization (Assinger, 2014). The rise in leukocytes primarily involved neutrophils, lymphocytes, and monocytes, representing a coordinated host response to detect and eliminate larvae. Thrombocytosis likely resulted from infection-induced cytokine signaling, particularly through interleukin-6 (IL-6)–mediated stimulation of megakaryocyte proliferation, enhancing platelet production during inflammation. These changes illustrate the dual role of the immune system in pathogen clearance and the potential for excessive inflammatory damage. Treatment with TCE normalized WBC and platelet counts, indicating suppression of hyperactive immune responses and restoration of hematopoietic balance. This immunomodulatory effect is likely mediated by downregulation of pro-inflammatory cytokines, including IL-1β, IL-6, and tumor necrosis factor-alpha (TNF-α), as well as modulation of the NF-κB pathway, thereby controlling leukocyte proliferation, limiting platelet overproduction, and promoting immune homeostasis. These results are consistent with previous studies showing that phenolic- and flavonoid-rich fungal extracts exert anti-inflammatory and immunoregulatory effects, alleviating infection-induced hematological disturbances (Liu *et al*., 2017).

H. thalassini L3 infection led to marked splenomegaly, evidenced by a significant increase in the spleen index, particularly in mice exposed to freshly collected larvae. This pathological enlargement reflects multiple processes, including enhanced erythrophagocytosis due to the destruction of damaged erythrocytes, lymphoid hyperplasia from B- and T-cell proliferation in response to persistent antigenic stimulation, and oxidative tissue injury from excessive ROS production during the host immune response (George *et al*., 2008; Bernal-Valle *et al*., 2022). The highest spleen indices were associated with heavier parasitic load, indicating that the extent of splenic hypertrophy correlates with infection intensity and immune activation. Histological examination revealed disrupted red and white pulp architecture, congestion, and inflammatory cell infiltration, confirming structural and functional compromise (Elsayed *et al*., 2019). Treatment with TCE significantly mitigated splenomegaly, lowering spleen indices and restoring histological architecture. This protective effect is likely attributable to TCE's antioxidant and cytoprotective properties, which reduce oxidative damage, stabilize cellular membranes, and preserve splenic microarchitecture. Furthermore, TCE may modulate immune-driven tissue remodeling by downregulating pro-inflammatory cytokines, reducing lymphoid hyperplasia, and enhancing endogenous antioxidant enzyme activity, thereby supporting splenic regeneration and functional homeostasis (Tejedor-Calvo *et al*., 2021).

Apoptotic responses in infected mice were thoroughly assessed using immunohistochemistry and quantitative gene-expression analysis of caspase-3, a key executioner enzyme that orchestrates the final stages of programmed cell death. In the spleens of mice infected with *H. thalassini* L3 larvae, caspase-3 expression was markedly elevated at both mRNA and protein levels, accompanied by intense immunoreactivity, indicating activation of intrinsic apoptotic pathways (Elsayed *et al*., 2019; Pawłowska *et al*., 2023). The apoptosis is likely driven by excessive ROS production, mitochondrial dysfunction, cytochrome c release, and disruption of redox balance, leading to caspase-dependent cell death (George *et al*., 2008; Al Quraishy *et al*., 2024). The effect was most pronounced in mice exposed to freshly collected L3 larvae, reflecting cumulative oxidative damage, progressive deterioration of splenic tissue, and impaired immune function (Kim *et al*., 2015). Treatment with TCE significantly suppressed caspase-3 expression and reduced immunohistochemical staining, demonstrating potent anti-apoptotic activity. This protection is likely mediated via ROS scavenging, stabilization of mitochondrial membranes, and modulation of transcriptional regulators of apoptosis and inflammation (Al-Laith, 2010; Tejedor-Calvo *et al*., 2021). Furthermore, TCE may inhibit TNF-α/NF-κB and p53-dependent pathways, limiting immune-mediated cell death and supporting splenic cellular survival (Liu *et al*., 2017). Similar protective effects of phenolic- and flavonoid-rich fungal extracts have been reported in hepatic and splenic tissues under chemical or parasitic stress, highlighting their role in mitigating oxidative injury, regulating immune responses, and preserving tissue architecture (Elsayed *et al*., 2019; Tejedor-Calvo *et al*., 2021).

Although the present study highlights the protective effects of TCE against *H. thalassini* L3 infection, it is subject to several limitations. These include the use of a murine model that may not fully represent natural host-parasite interactions, reliance on a crude extract without characterization of individual bioactive constituents, a relatively short experimental period focused primarily on acute effects, the absence of in-depth molecular analyses of cytokines and signaling pathways, and possible variability in parasitic burden and host biochemical responses.

Limitations of the study

It should be noted that the experimental approach used in this study relied on crude extracts of *H. thalassini* third-stage larvae rather than on live-larval exposure. While this strategy allows for standardized antigen administration and facilitates evaluation of host immune-related, oxidative, and apoptosis-associated responses to anisakid antigens, it does not fully capture the biological com-

plexity of natural anisakid infection. Specifically, essential aspects of live infection—such as larval migration, tissue penetration, mechanical tissue damage, and dynamic host–parasite interactions—are not represented in this model and may contribute significantly to disease pathogenesis under natural conditions. Accordingly, although the current findings offer valuable insight into the antioxidant and partial immunomodulatory effects of *T. claveryi* extract in anisakid antigen–induced pathology, additional studies employing live larval challenge models and extended experimental timelines are warranted to more closely simulate natural infection and enhance the translational relevance of these results. In addition, the lack of compound-specific phytochemical characterization limits the ability to definitively attribute the observed biological activities to individual bioactive constituents. Furthermore, immune modulation in this study was evaluated using indirect indicators; therefore, future investigations incorporating cytokine profiling, immune cell subset characterization, and molecular immune signaling analyses are necessary to achieve a more comprehensive understanding of the immunomodulatory mechanisms of *T. claveryi* extract.

Conclusion

This study provides evidence that the *T. claveryi* extract exhibits pronounced antioxidant activity, along with partial immunomodulatory, hematoprotective, and anti-apoptotic effects, in a murine model of *H. thalassini* L3–induced pathology. Treatment with the extract alleviated infection-related oxidative stress, corrected hematological alterations, attenuated splenic enlargement, and downregulated Caspase-3 expression at both mRNA and protein levels, reflecting reduced apoptotic activity and moderation of immune-associated disturbances. The observed protective actions are likely attributable to the extract's overall bioactive profile, which has been previously reported to contain phenolic compounds, flavonoids, and other antioxidant metabolites. Nonetheless, because compound-specific phytochemical characterization was not conducted in the present investigation, the precise contribution of individual constituents cannot be definitively established. Consequently, future studies employing advanced analytical approaches, including HPLC or LC–MS, are required to identify and quantify the active molecules underlying these biological effects. Such investigations will be critical for clarifying the mechanistic basis of *T. claveryi* bioactivity and for supporting its prospective application as a natural therapeutic agent in the management of fishborne anisakid-related oxidative stress and immune-mediated pathology.

Acknowledgments

This study was supported by the Ongoing Research Funding Program (ORF-2026-25), King Saud University, Riyadh, Saudi Arabia; and Princess Nourah bint Abdulrahman University Researchers Supporting Project number (PNURSP2026R931), Princess Nourah bint Abdulrahman University, Riyadh, Saudi Arabia.

Availability of data and materials

All the datasets analyzed during this study are included in this published article.

Conoflict of Interest

The author(s) declare that they have no conflict of interest regarding the content of this article.

Consent to Participate

All authors agreed to participate in this study.

Consent to Publish

All authors agreed to publish the data in this study.

References

Abbas, M.T. (2019): The prophylactic and protective effects of *Terfezia claveryi* extracts on ibuprofen-induced oxidative stress in pregnant rats. *Gazi Med J*, 30(3): 273 – 278

Abdel-Gaber, R., Alojayri, G., Al-Quraishy, S., Al-Shaebi, E.M., Mohammed, O.B. (2024): Morphological and molecular studies of *Hysterothylacium thalassini* third-stage larvae (Ascaridida, Raphidascarididae) in the greater lizardfish *Saurida tumbil*. *Arq Bras Med Vet Zootec*, 76(4): e13206. DOI: 10.1590/1678-4162-13206

Al-Laith, A.A.A. (2010): Antioxidant components and antioxidant/antiradical activities of desert truffle (*Tirmania nivea*) from various Middle Eastern origins. *J Food Compos Anal*, 23: 15 – 22. DOI: 10.1016/j.jfca.2009.07.005

Al-Quraishy, S., Abdel-Gaber, R., Alamari, G., Meryk, A., El-Ashram, S., Al-Shaebi, E.M., Dkhil, M.A. (2024): Fighting eimeriosis by using the anti-eimerial and anti-apoptotic properties of rhatany root extract. *Front Immunol*, 15: 1 430 960. DOI: 10.3389/fimmu.2024.1430960

Assinger, A. (2014): Platelets and infection – an emerging role of platelets in viral infection. *Front Immunol*, 5: 649. DOI: 10.3389/fimmu.2014.00649

Audicana, M.T., Ansotegui, I.J., De Corres, L.F., Kennedy, M.W. (2002): *Anisakis simplex*: Dangerous – dead and alive?. *Trends Parasitol*, 18: 20 – 25. DOI: 10.1016/s1471-4922(01)02152-3

Baliyan, S., Mukherjee, R., Priyadarshini, A., Vibhuti, A., Gupta, A., Pandey, R.P., Chang, C.-M. (2022): Determination of antioxidants by DPPH radical scavenging activity and quantitative phytochemical analysis of *Ficus religiosa*. *Molecules*, 27(4): 1326. DOI: 10.3390/molecules27041326

Bauomy, A.A., Dkhil, M.A., Diab, M.S.M., Amer, O.S.O., Al-Quraishy, S. (2014): Response of spleen and jejunum of mice infected with *Schistosoma mansoni* to mulberry treatment. *Pak J Zool*, 46(3): 753 – 761

Benzie, I.F., Strain, J.J. (1996): The ferric reducing ability of plasma (FRAP) as a measure of "antioxidant power": the FRAP assay. *Anal Biochem*, 239(1): 70 – 76. DOI: 10.1006/abio.1996.0292

Bernal-Valle, S., Teixeira, M.N., de Araújo Neto, A.R., Gonçalves-Souza, T., Feitoza, B.F., Dos Santos, S.M., da Silva, A.J., da Silva, R.J., de Oliveira, M.A.B., de Oliveira, J.B. (2022): Parasitic infections, hematological and biochemical parameters suggest appropriate health status of wild coati populations in anthropic Atlantic Forest remnants. *Vet Parasitol Reg Stud Rep*, 30: 100693. DOI: 10.1016/j.vprsr.2022.100693

Chai, J.Y., Sohn, W.M., Jung, B.K. (2024): Anisakidosis in humans and animals and detection of anisakid larvae in fish and cephalopods in Korea: A literature review (1971 – 2022). *Ann Clin Microbiol*, 27(2): 93 – 130. DOI: 10.5145/ACM.2024.27.2.6

Dela Cruz, T.T.M., Llanes, K.K.R., Toledo, J.M.S., Catabay, J.A., Fornillos, R.J.C., Fontanilla, I.K.C., Paller, V.G.V. (2022): Prevalence and molecular characterization of ascaridoid parasites of Philippine *Decapterus* species. *J Nematol*, 54(1): 1 – 10. DOI: 10.2478/jofnem-2022-0030

Dkhil, M.A., Aljawdah, H.M.A., Abdel-Gaber, R., Thagfan, F.A., Delic, D., Al-Quraishy, S. (2023): The effect of *Eucalyptus camaldulensis* leaf extracts from different environmental harvesting locations on *Plasmodium chabaudi*-induced malaria outcome. *Food Sci Technol Campinas*, 43: e006723. DOI: 10.1590/fst.006723

Elsayed, E.A., Alsahli, F.D., Barakat, I.A., El Enshasy, H.A., Wadaan, M.A. (2019): Assessment of in vitro antimicrobial and anti-breast cancer activities of extracts isolated from desert truffles in Saudi Arabia. *J Sci Ind Res*, 78: 419 – 425.

George, J.F., Braun, A., Brusko, T.M., Joseph, R., Bolisetty, S., Wasserfall, C.H., Atkinson, M.A., Agarwal, A., Kapturczak, M.H. (2008): Suppression by CD4+CD25+ regulatory T cells is dependent on expression of heme oxygenase-1 in antigen-presenting cells. *Am J Pathol*, 173(1): 154 – 160. DOI: 10.2353/ajpath.2008.070963

Guenane, H., Bakchiche, B., Erenler, R., Yildiz, I., Mohamed, A.S., El-Shazly, M.A.M. (2024): Mineral contents, antioxidant and antimicrobial activities of Algerian *Terfezia claveryi* extracts. *Fabad J Pharm Sci,* 49(1): 19 – 36. DOI: 10.55262/fabadeczacilik.1326710

Iglesias, R., Leiro, J., Ubeira, F.M., Santamarina, M.T., Navarrete, I., Sanmartín, M.L. (1996): Antigenic cross-reactivity in mice between third-stage larvae of *Anisakis simplex* and other nematodes. *Parasitol Res*, 82: 378 – 381. DOI: 10.1007/s004360050131

İşlek, C., Saridoğan, B.G.O., Sevindik, M., Akata, I. (2021): Biological activities and heavy metal contents of some *Pholiota* species. *Fresen Environ Bull*, 30(6): 6109 – 6114

Janakat, S., Nassar, M. (2010): Hepatoprotective activity of desert truffle (*Terfezia claveryi*) in comparison with the effect of *Nigella sativa* in the rat. *Pak J Nutr*, 9(1): 52 – 56. DOI: 10.3923/pjn.2010.52.56

Kim, S. H., Jakhar, R., Kang, S.C. (2015): Apoptotic properties of polysaccharide isolated from fruiting bodies of medicinal mushroom *Fomes fomentarius* in human lung carcinoma cell line. *Saudi J Biol Sci*, 22(4): 484 – 490. DOI: 10.1016/j.sjbs.2014.11.022

Kivrak, Ş., Göktürk, T., Kivrak, İ., Kaya, E., Karababa, E. (2019): Investigation of phenolic profiles and antioxidant activities of some *Salvia* species commonly grown in Southwest Anatolia using UP-LC-ESI-MS/MS. *Food Sci Technol*, *Campinas,* 39(2): 423 – 431. DOI: 10.1590/fst.32017

Li, L., Xu, Z., Zhang, L. (2007) A new species of genus *Hysterothylacium* Ward et Magath, 1917 (Nematoda, Anisakidae) from *Liparis tanakae* (Scorpaeniformes, Liparidae) from the Yellow Sea, China. *Acta Parasitol*, 52(4): 371 – 375. DOI: 10.2478/s11686-007-0046-8

Liu, T., Zhang, L., Joo, D., Sun, S.-C. (2017): NF-κB signaling in inflammation. *Signal Transduct Target Ther*, 2: 17023. DOI: 10.1038/sigtrans.2017.23

Livak, K.J., Schmittgen, T.D. (2001): Analysis of relative gene expression data using real-time quantitative PCR and the 2−ΔΔCT method. *Methods*, 25(4): 402 – 408. DOI: 10.1006/meth.2001.1262

Menshawy, S., Essa, B., Shaaban, S., Zaid, A.A., AbouLaila, M., Wheeb, H. (2024): Prevalence and molecular characterization of *Hysterothylacium* species infecting *Pandora* (*Pagellus erythrinus*) in the Mediterranean Sea of Egypt. *Vet Parasitol Reg Stud Rep*, 52: 101037. DOI: 10.1016/j.vprsr.2024.101037

Pawłowska, M., Mila-Kierzenkowska, C., Szczegielniak, J., Woźniak, A. (2023): Oxidative stress in parasitic diseases—Reactive oxygen species as mediators of interactions between the host and the parasites. *Antioxidants*, 13(1): 38. DOI: 10.3390/antiox13010038

Re, R., Pellegrini, N., Proteggente, A., Pannala, A., Yang, M., Rice-Evans, C. (1999) Antioxidant activity applying an improved ABTS radical cation decolorization assay. *Free Radic Biol Med*, 26(9–10): 1231 – 1237. DOI: 10.1016/S0891-5849(98)00315-3

Souna, M., Tefiani, C., Azz I, R., Chaouche, T.M. (2023): Myco-Chemical Constituents and Anti-Inflammatory Activity of *Terfezia claveryi* Chatin from Algeria. *Biol Life Sci Forum,* 27

Souna, M., Tefiani, C., Azzi, R., Chaouche, T.M., Habi, S. (2023): Mycochemical constituents and anti-inflammatory activity of *Terfezia claveryi* Chatin from Algeria. *Biol Life Sci Forum*, 27(1): 19. DOI: 10.3390/IECAG2023-14980

Tejedor-Calvo, E., Amara, K., Reis, F.S., Barros, L., Martins, A., Calhelha, R.C., Venturini, M.E., Blanco, D., Redondo, D., Marco, P., Ferreira, I.C. (2021): Chemical composition and evaluation of antioxidant, antimicrobial and antiproliferative activities of *Tuber* and *Terfezia* truffles. *Food Res Int*, 140: 110071. DOI: 10.1016/j.foodres.2020.110071

Veeraraghavan, V.P., Hussain, S., Balakrishna, J.P., Dhawale, L., Kullappan, M., Ambrose, J.M., Mohan, S.K. (2021): A comparative and critical review on ethnopharmacological importance of desert truffles: *Terfezia claveryi*, *Terfezia boudieri*, and *Tirmania nivea*. *Food Rev Int*, 1 – 21. DOI: 10.1080/87559129.2021.1889581